

Going green: The application of magnetic fields (see figure), pH and thermoresponsive materials, molecular antisolvents, or nanostructured colloidal solvents provide effective and efficient methodologies for recycling nanoparticles without significant costs, time demands, or energy consumption. Recent advances in strategies for recycling and reusing functional nanomaterials are described.



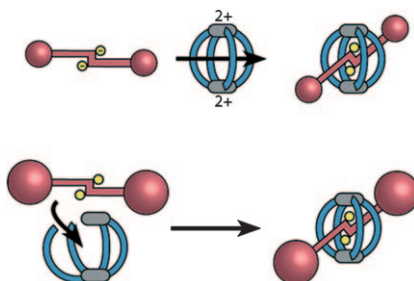
Nanomaterials

*O. Myakonkaya, Z. Hu, M. F. Nazar, J. Eastoe** 11784–11790

Recycling Functional Colloids and Nanoparticles

COMMUNICATIONS

Please let me in! A new kind of (pseudo)rotaxane is formed quantitatively when a bis-anionic thread is added to a molecular cage comprised of two positively charged metal complexes. The rotaxation mechanism follows two alternative ways depending on the metal (Pd vs. Pt) and the stopper size of the guest (see figure).



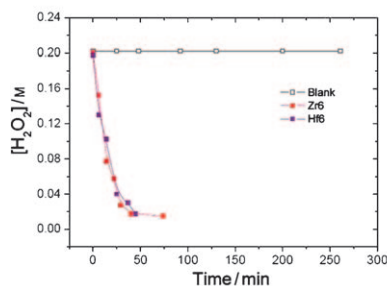
Host–Guest Systems

*G. H. Clever, M. Shionoya** 11792–11796

A pH Switchable Pseudorotaxane based on a Metal Cage and a Bis-anionic Thread



Six of the best! Two Zr₆- and Hf₆-containing tungstoarsenates(III) [M₆O₄(OH)₄(H₂O)₂(CH₃COO)₅-(AsW₅O₃₃)₂]¹¹⁻ (M = Zr, Hf) have been synthesized and structurally characterized in solution and in the solid state, and both species are highly active in H₂O₂-based selective oxidations.



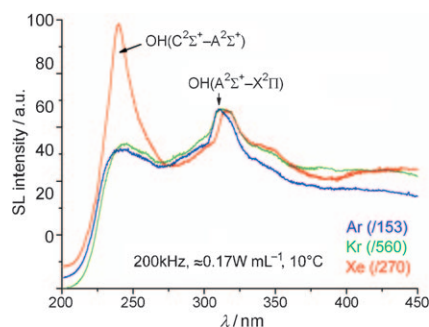
Polyoxometalates

G. Al-Kadamany, S. S. Mal, B. Milev, B. G. Donoeva, R. I. Maksimovskaya, O. A. Kholdeeva, U. Kortz** 11797–11800

Hexazirconium- and Hexahafnium-Containing Tungstoarsenates(III) and Their Oxidation Catalysis Properties



Bubble trouble: Multibubble sonoluminescence spectra in water under Kr and Xe present emission lines of OH(C²Σ⁺–A²Σ⁺) (see graphic). This band, never observed in flames, indicates plasma formation in the collapsing bubbles.



Sonoluminescence

R. Pflieger, H.-P. Brau, S. I. Nikitenko* 11801–11803

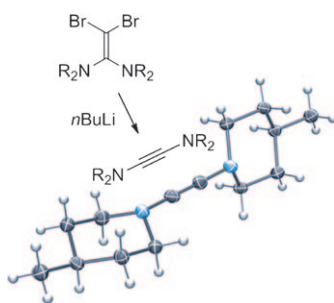
Sonoluminescence from OH(C²Σ⁺) and OH(A²Σ⁺) Radicals in Water: Evidence for Plasma Formation during Multibubble Cavitation



Diaminoalkynes

A. R. Petrov, C. G. Daniliuc,
P. G. Jones, M. Tamm* . . 11804–11808

A Novel Synthetic Approach to Diaminoacetylenes: Structural Characterization and Reactivity of Aromatic and Aliphatic Ynediamines

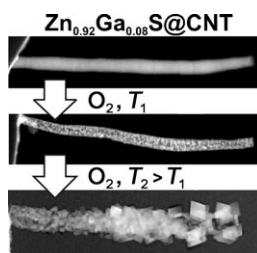


Electron-rich diaminoalkynes with a variable substitution pattern can be conveniently prepared by lithiation of 2,2-dibromo-1,1-ethenediamines; the alkynes are formed by a Fritsch–Buttenberg–Wiechell rearrangement of intermediate LiBr–vinylidene species. The first two X-ray crystal structures of diaminoalkynes are presented, which show almost perpendicular orientations of the NC_3 planes.

Electron Microscopy

P. M. F. J. Costa,* T. W. Hansen,
J. B. Wagner,
R. E. Dunin-Borkowski . . 11809–11812

Imaging the Oxidation of ZnS Encapsulated in Carbon Nanotubes

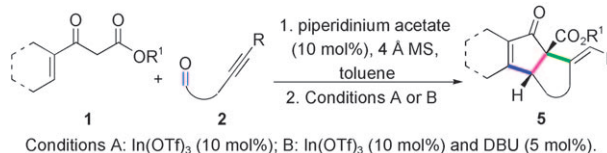


Cable-to-tube transition: Core–shell sulfide–carbon nanocables have been oxidised to hollow polycrystalline nanowires and further assembled to crystallites inside a transmission electron microscope. The full experimental life cycle (see graphic) was followed for a single nanostructure; this provided extended structural and chemical information that supports a nanocable-to-nanotube transition and the presence of the Kirkendall effect.

Polycyclic Compounds

L. Liu, L. Wei, Y. Lu,
J. Zhang* 11813–11817

One-Pot Tandem Catalysis: A Concise Route to Fused Bicyclic Scaffolds from Acyclic β -Ketoesters and Alkynyl Aldehydes



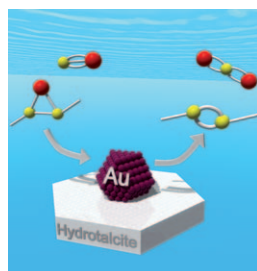
“Quick-step” synthesis: A rapid and highly efficient route to fused polycyclic scaffolds from simple, readily available β -ketoesters and alkynyl aldehydes was developed (see scheme) as a one-pot reaction by combining

three fundamental reactions, that is, the Knoevenagel condensation, Nazarov cyclization, and Conia-ene reactions. Piperidinium acetate was found to be a tandem catalyst in these one-pot reactions.

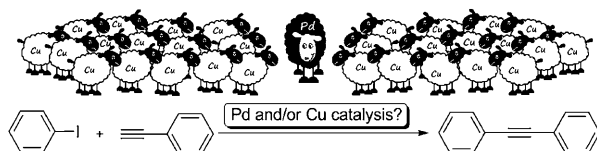
Heterogeneous Catalysis

T. Mitsudome, A. Noujima, Y. Mikami,
T. Mizugaki, K. Jitsukawa,
K. Kaneda* 11818–11821

Room-Temperature Deoxygenation of Epoxides with CO Catalyzed by Hydrotalcite-Supported Gold Nanoparticles in Water



Epoxide deoxygenation: Hydrotalcite-supported gold nanoparticles (Au/HT) efficiently catalyze the deoxygenation of epoxides to alkenes in water at room temperature under CO at atmospheric pressure and in the absence of organic solvents (see graphic). Moreover, Au/HT retains its activity and selectivity and can be reused.



Palladacadabra! The effect of ppb levels of palladium on the “copper-catalyzed” Sonogashira coupling is reported. The observed high sensitivity

to palladium impurities queries the existence of pure copper catalysis in the coupling of aryl iodides and terminal acetylenes (see figure).

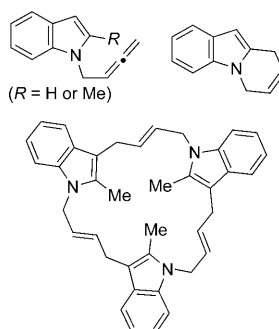
Cross-Coupling Reactions

Z. Gonda, G. L. Tolnai,
Z. Novák* 11822–11826

Dramatic Impact of ppb Levels of Palladium on the “Copper-Catalyzed” Sonogashira Coupling



Gold-ringing! Modification of the substitution at C2 drives an entirely different cyclization of *N*-tethered allenylindoles. An efficient cycloisomerization takes place for the case of *R* being hydrogen, that is, compatible with additional functional groups. A methyl at C2 precludes this possibility and launches a stepwise process that can be tuned to yield macrocyclic trimers.



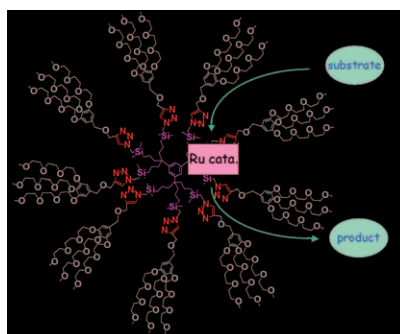
Gold Catalysis

J. Barluenga,* M. Piedrafita,
A. Ballesteros, Á. L. Suárez-Sobrino,
J. M. González 11827–11831

Gold-Catalyzed Annulations of 1-(2,3-Butadienyl)-1*H*-Indole Derivatives



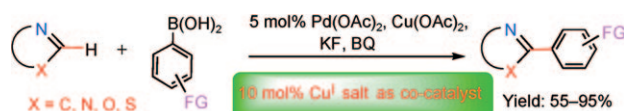
A dendritic nanoreactor (see graphic) constructed by 1→3 connectivity and terminated by 27 tetraethyleneglycol tethers induces ring-closing metathesis (RCM), cross metathesis (CM) and enyne metathesis (EYM) using low amounts of Grubbs-II catalyst in water and air, down to 0.04% Grubbs catalyst for RCM. The dendrimer can be re-used at least 10 times without significant yield decrease.



Heterogeneous Catalysis

A. K. Diallo, E. Boisselier, L. Liang,
J. Ruiz, D. Astruc* 11832–11835

Dendrimer-Induced Molecular Catalysis in Water: The Example of Olefin Metathesis



Bimetallic catalytic system: Palladium/copper bimetallic-catalyzed Suzuki–Miyaura-type coupling has been disclosed for direct C–H arylation of

azoles, instead of azole halides or pseudohalides, with arylboronic acids (see scheme).

Bimetallic Catalysis

B. Liu, X. Qin, K. Li, X. Li, Q. Guo,
J. Lan, J. You* 11836–11839

A Palladium/Copper Bimetallic Catalytic System: Dramatic Improvement for Suzuki–Miyaura-Type Direct C–H Arylation of Azoles with Arylboronic Acids



A general and practical synthesis of (*E*)- α,β -unsaturated esters and ketones was achieved by the reaction of carbonyl compounds with ethyl-4,4,4-trifluoroacetate and trifluoro-substi-

tuted 1,3-diketones in the presence of piperidine in dichloromethane at room temperature ($\approx 40^\circ\text{C}$) with excellent stereoselectivity (see scheme).

Synthetic Methods


B. China Raju,*
P. Suman 11840–11842

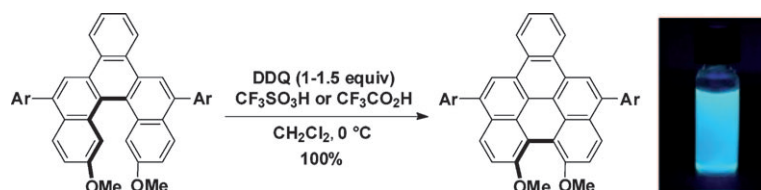
New and Facile Approach for the Synthesis of (*E*)- α,β -Unsaturated Esters and Ketones



Helical Structures

*J.-D. Chen, H.-Y. Lu,
C.-F. Chen** 11843–11846

 **Synthesis and Structures of Multifunctionalized Helicenes and Dehydrohelicenes: An Efficient Route to Construct Cyan Fluorescent Molecules**



Spiral up! A series of multifunctionalized benzo[5]helicene derivatives and a benzo[7]helicene were conveniently synthesized. Moreover, the oxidative cyclodehydrogenation of the benzo[5]helicenes by DDQ in trifluoroacetic

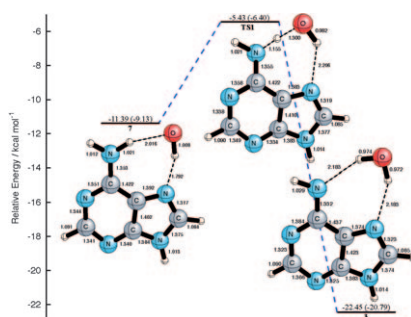
acid or trifluoromethanesulfonic acid quantitatively provided the corresponding dehydro[5]helicene derivatives, which showed the cyan fluorescent properties (shown here).

FULL PAPERS

Radical Reactions

*Q. Cheng, J. Gu, K. R. Compaan,
H. F. Schaefer, III** 11848–11858


Hydroxyl Radical Reactions with Adenine: Reactant Complexes, Transition States, and Product Complexes

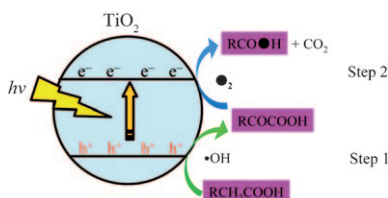


Sixth sense! Six possible dehydrogenation reaction pathways for adenine attacked by the hydroxyl radical have been investigated at the B3LYP/DZP++ level of theory. The N₆-position is most favorable for OH radical attack, leading to formation of N₆-dehydrogenated adenine radicals (see graphic).

Photocatalysis

B. Wen, Y. Li, C. Chen, W. Ma,
J. Zhao** 11859–11866

 **An Unexplored O₂-Involved Pathway for the Decarboxylation of Saturated Carboxylic Acids by TiO₂ Photocatalysis: An Isotopic Probe Study**

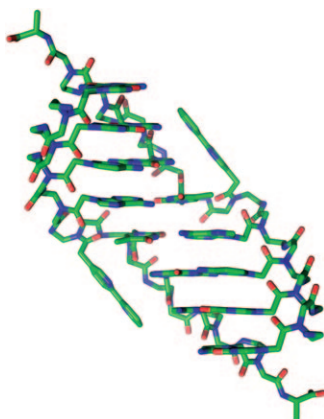


Acid aerobics! An O₂-involved pathway for the decarboxylation of saturated carboxylic acids by TiO₂ photocatalysis is clarified, and has been found to be composed of two major tandem steps. An oxygen atom of O₂ is incorporated into the product acid in the second step (see scheme).

PNA Duplexes

J. I. Yeh, E. Pohl, D. Truan, W. He,
G. M. Sheldrick, S. Du,
C. Achim** 11867–11875

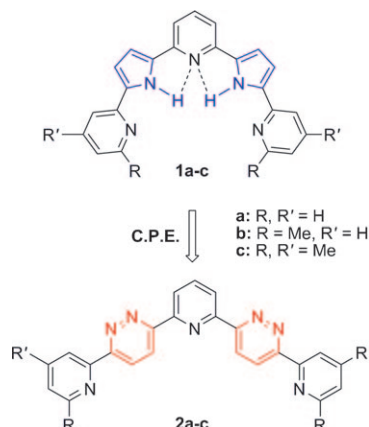
 **The Crystal Structure of Non-Modified and Bipyridine-Modified PNA Duplexes**



Inside out: The comparative study of the crystal structure of two peptide nucleic acid (PNA) duplexes that differ by the presence of a central pair of bipyridine ligands shows that the ligands are extruded from the duplex, which induces a prominent bending of the PNA (see figure).

Electrochemical pyrrole synthesis:

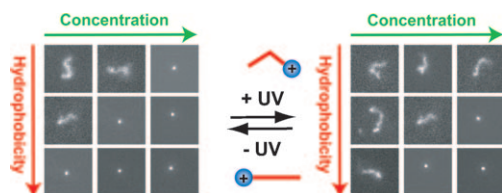
Donor–acceptor pyridine–pyrrole molecular strands **1** composed of two electron-rich pyrrole units sandwiched between pyridinic cores were synthesized by electroreduction of alternating tripyridyl–bipyridazine precursors **2** (see picture). The absorption behavior of the tripyridyl–dipyrrole ligands and their structures in the solid state were evaluated and compared to theoretical calculations. C.P.E. = controlled-potential electrolysis.



Molecular Strands

A. Tabatchnik-Rebillon, C. Aubé, H. Bakkali, T. Delaunay, G. T. Manh, V. Blot, C. Thobie-Gautier, E. Renault, M. Soulard, A. Planchat, J.-Y. Le Questel, R. Le Guével, C. Guguen-Guillouzo, B. Kauffmann, Y. Ferrand, I. Huc, K. Urgan, S. Condon, E. Léonel, M. Evain, J. Lebreton, D. Jacquemin, M. Pipelier, D. Dubreuil* 11876–11889

Electrochemical Synthesis and Characterisation of Alternating Tripyridyl–Dipyrrole Molecular Strands with Multiple Nitrogen-Based Donor–Acceptor Binding Sites



Photocontrol: The synthesis and characterisation of photosensitive cationic surfactants with varying hydrophobic tail lengths (AzoCx) for the photocontrol of DNA conformation is described. These molecules induce photodependent DNA compaction, originating

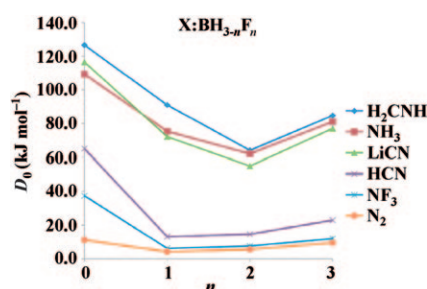
in the photodependent polarities of their hydrophobic tails. Optimum performance was achieved with AzoC5, which allowed reversible control of DNA conformation with light at a concentration seven times smaller than previously reported (see figure).

DNA Conformation

A. Diguët, N. K. Mani, M. Geoffroy, M. Sollogoub, D. Baigt* 11890–11896

Photosensitive Surfactants with Various Hydrophobic Tail Lengths for the Photocontrol of Genomic DNA Conformation with Improved Efficiency

Understanding bonding: B–N bonding in complexes $X: \text{BH}_{3-n}\text{F}_n$ and $X: \text{BH}_{3-n}\text{Cl}_n$ presents a challenge for previously proposed models, which fail to explain the stability trends in these complexes as a function of the number of halogen atoms in the Lewis acids (see figure). Acid deformation plays a key role in determining these trends.

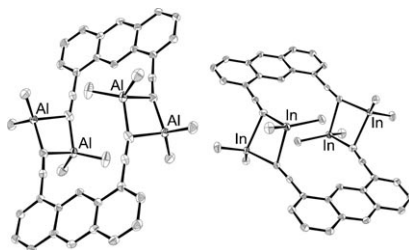


Acid Deformation

I. Alkorta, J. Elguero, J. E. Del Bene, O. Mó, M. Yáñez* 11897–11905

New Insights into Factors Influencing B–N Bonding in $X: \text{BH}_{3-n}\text{F}_n$ and $X: \text{BH}_{3-n}\text{Cl}_n$ for $X = \text{N}_2, \text{HCN}, \text{LiCN}, \text{H}_2\text{CNH}, \text{NF}_3, \text{NH}_3$ and $n = 0-3$: The Importance of Deformation

Moving four-ward: Four Lewis acidic metal atoms held together by rigid hydrocarbon frameworks can be synthesised from 1,8-diethynylantracene with metal alkyls MR_3 (M = Al, Ga, In; R = Me, Et) under alkane elimination (see figure). The arrangement of four close-lying metal functions is broken up in donor solvents like THF.



Lewis Acids

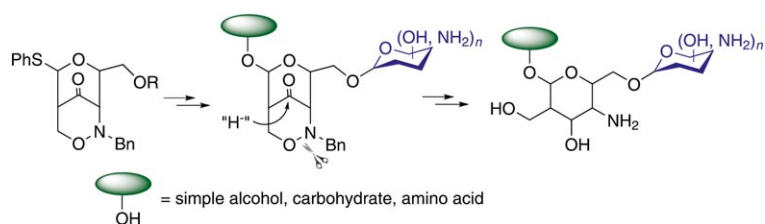
J. Chmiel, B. Neumann, H.-G. Stammer, N. W. Mitzel* 11906–11914

Dialkylaluminium-, -Gallium-, and -Indium-Based Poly-Lewis Acids with a 1,8-Diethynylantracene Backbone

Carbohydrate Derivatives

F. Pfrenge,
H.-U. Reissig* 11915–11925

Internally Protected Amino Sugar Equivalents from Enantiopure 1,2-Oxazines: Synthesis of Variably Configured Carbohydrates with C-Branched Amino Sugar Units



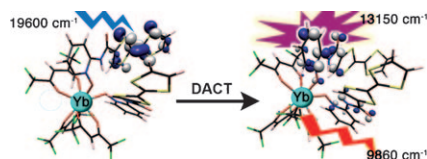
Make it simple: A Lewis acid mediated rearrangement of 1,2-oxazines delivers internally protected amino sugar equivalents that can be incorporated into oligosaccharides. Deprotection of the amino sugar precursors by

simple reductive steps provides new natural product analogues having C2-branched 4-amino sugar units with different absolute and relative configurations.

Luminescence

F. Pointillart, T. Cauchy, O. Maury,
Y. Le Gal, S. Golhen, O. Cador,
L. Ouahab* 11926–11941

Tetrathiafulvalene-amido-2-pyridine-N-oxide as Efficient Charge-Transfer Antenna Ligand for the Sensitization of Yb^{III} Luminescence in a Series of Lanthanide Paramagnetic Coordination Complexes

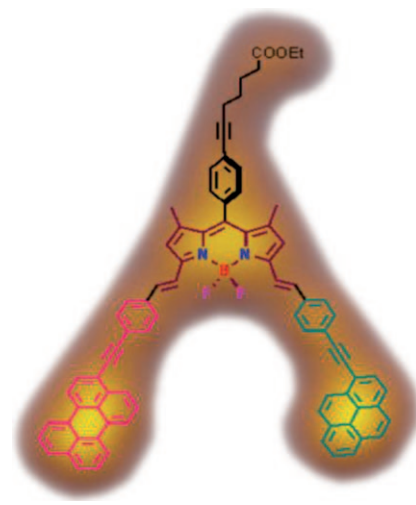


Efficient antenna: Three structural families of complexes of diverse ionic radii lanthanide ions that involve tetrathiafulvalene-amido-2-pyridine-N-oxide ligands (L) have been structurally, electrochemically, magnetically, and optically studied. The IR luminescence of a Yb complex can be sensitized by an L antenna effect (see image; DACT = donor-to-acceptor charge transfer).

Extended Chromophores

R. Ziessel,* S. Rihn,
A. Harriman* 11942–11953

Quasi-One-Dimensional Electronic Systems Formed from Boron Dipyrromethene (BODIPY) Dyes

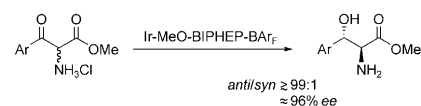


Getting bigger all the time! Appending aryl polycycles to an expanded boron dipyrromethene nucleus leads to giant chromophores that emit at long wavelengths, while absorbing over most of the visible region (see figure). All spectroscopic indicators point to a shared electronic system that is fully delocalised over the π system. These new materials hold promise for use as organic solar concentrators or in light-conversion devices.

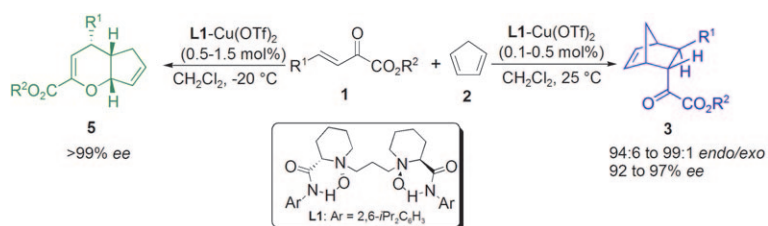
Asymmetric Hydrogenation

T. Maeda, K. Makino, M. Iwasaki,
Y. Hamada* 11954–11962

Diastereo- and Enantioselective Hydrogenation of α-Amino-β-Keto Ester Hydrochlorides Catalyzed by an Iridium Complex with MeO-BIPHEP and NaBAR_F: Catalytic Cycle and Five-Membered Chelation Mechanism of Asymmetric Hydrogenation



Apply some pressure: The Ir-catalyzed asymmetric hydrogenation of α-amino-β-keto ester hydrochlorides proceeds through a dynamic kinetic resolution to produce anti-β-hydroxy-α-amino acid esters in a high diastereo- and enantioselective manner (see scheme). Mechanistic studies revealed that this unique asymmetric hydrogenation proceeds through reduction of the ketone moiety via the five-membered transition state.



Temperature control: Asymmetric (hetero-)Diels–Alder reactions of β,γ -unsaturated α -ketoesters with cyclopentadiene promoted by an N,N' -dioxide–Cu(OTf)₂ complex afforded the

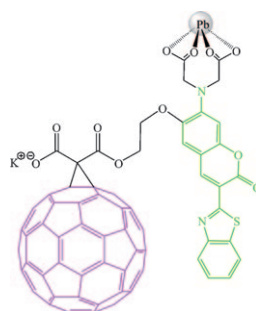
products with excellent *endo/exo* ratios and enantioselectivities (see scheme; Tf = triflate). The chemoselectivity could be controlled by regulating the reaction temperature.

Asymmetric Reactions

Y. Zhu, X. Chen, M. Xie, S. Dong, Z. Qiao, L. Lin, X. Liu, X. Feng* 11963–11968

Asymmetric Diels–Alder and Inverse-Electron-Demand Hetero-Diels–Alder Reactions of β,γ -Unsaturated α -Ketoesters with Cyclopentadiene Catalyzed by N,N' -Dioxide Copper(II) Complex

Lead along by fullerene: A coumarin derivative with a malonate unit has been synthesized and used for the preparation of a fullerene–coumarin dyad through the Bingel cyclopropanation method (see scheme). The dyad was tested as a metal receptor for divalent metal cations and showed binding selectivity for lead ions.

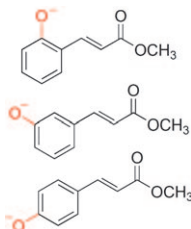


Dyes/Pigments

G. Pagona, S. P. Economopoulos, G. K. Tsikalas, H. E. Katerinopoulos, N. Tagmatarchis* 11969–11976

Fullerene–Coumarin Dyad as a Selective Metal Receptor: Synthesis, Photo-physical Properties, Electrochemistry and Ion Binding Studies

This way and that way: The relevance of the push–pull system in the photo-absorption of the cofactor of photoactive yellow protein has been investigated through the measurement of the absorption spectra and theoretical calculations of the deprotonated *trans* *ortho*-, *meta*- and *para*-methyl coumarates (see scheme).

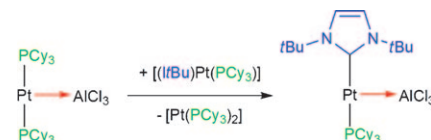


Push–Pull Systems

T. Rocha-Rinza,* O. Christiansen, D. B. Rahbek, B. Klærke, L. H. Andersen, K. Lincke, M. Brøndsted Nielsen 11977–11984

Spectroscopic Implications of the Electron Donor–Acceptor Effect in the Photoactive Yellow Protein Chromophore

Hitting the right note: The influence on the Lewis basic properties of platinum(0) complexes by exchange of phosphanes with N-heterocyclic carbenes (NHC) was investigated by synthesis of three related platinum–alane adducts (see graphic). The results of the theoretical investigations were validated by an unprecedented transfer experiment.

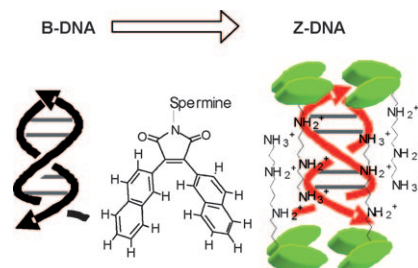


Platinum Complexes

J. Bauer, H. Braunschweig,* P. Brenner, K. Kraft, K. Radacki, K. Schwab 11985–11992

Late-Transition-Metal Complexes as Tunable Lewis Bases

From B to Z: The bis(2-naphthyl)-maleimide–spermine conjugate shown in the figure exhibits a remarkable ability to cause the B→Z transition of d(CGCGCG)₂ at low salt concentrations. A stable intermediate between the B and Z forms was observed in the presence of the ligand at about pH 8.



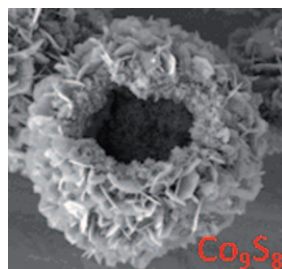
DNA Binding

I. Doi, G. Tsuji, K. Kawakami, O. Nakagawa, Y. Taniguchi, S. Sasaki* 11993–11999

The Spermine–Bisaryl Conjugate as a Potent Inducer of B- to Z-DNA Transition

Oxygen Reduction Reaction

Y.-X. Zhou, H.-B. Yao, Y. Wang,
H.-L. Liu, M.-R. Gao, P.-K. Shen,
S.-H. Yu* 12000–12007

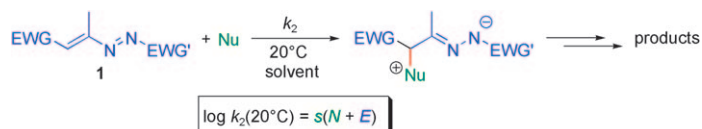


Cathode materials: Hierarchical hollow Co_9S_8 microspheres (shown here) can be synthesized by a simple solvothermal route in a binary solution of triethylenetetramine and deionized water. The onset potential of Co_9S_8 hollow spheres is 0.88 V for the oxygen reduction reaction. The magnetic properties of Co_9S_8 hollow microspheres and their use as cathode materials for lithium ion cells have been studied.

Hierarchical Hollow Co_9S_8 Microspheres: Solvothermal Synthesis, Magnetic, Electrochemical, and Electrocatalytic Properties

Kinetics

T. Kanzian, S. Nicolini,
L. De Crescentini, O. A. Attanasi,*
A. R. Ofial,* H. Mayr 12008–12016



Electrophilic Reactivities of 1,2-Diaza-1,3-dienes

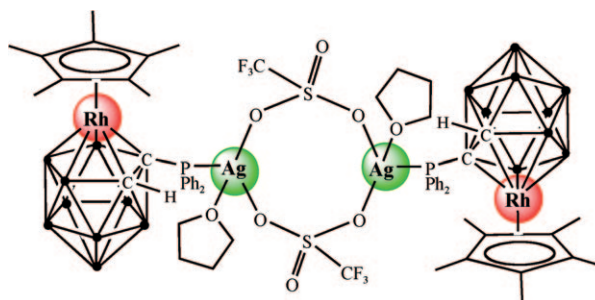
Electrophilicities quantified: The kinetics of the reactions of 1,2-diaza-1,3-dienes **1** with carbanions have been studied photometrically at 20 °C (see figure). The second-order rate constants were used to calculate the electrophilicity parameters E of com-

pounds **1** according to the linear free energy relationship $\log k_2(20^\circ\text{C}) = s(N + E)$. These parameters were employed to define the scope and limitations of the reactions of 1,2-diaza-1,3-dienes **1** with various nucleophiles.

Coordination Modes

X.-K. Huo, G. Su,
G.-X. Jin* 12017–12027

The Versatile Coordination Modes of Monophosphine-*o*-Carborane in the Formation of Iridium and Rhodium Complexes: Synthesis, Reactivity, and Characterization



A competitive coordinator: A series of organometallic complexes that contain monophosphine-*o*-carborane have been synthesized and structurally characterized through structure transitions

driven by these competitive coordination modes under different reaction conditions (an example of which is depicted). The influences of other factors were also explored preliminarily.

* Author to whom correspondence should be addressed

Supporting information on the WWW (see article for access details).

VIP Full Papers labeled with this symbol have been judged by two referees as being “very important papers”.

Video A video clip is available as Supporting Information on the WWW (see article for access details).

SERVICE

Spotlights 11780 Author Index 12028 Keyword Index 12029 Preview 12031

Issue 38/2010 was published online on September 29, 2010